ChemMedChem

ResearchArticle
doi.org/10.1002/cmdc.202200046

Chemistry Europe
European Chemical Societies Publishing

www.chemmedchem.org

VIP *Very Important Paper*

Anthracene-Walled Acyclic CB[n] Receptors: *in vitro* and *in vivo* Binding Properties toward Drugs of Abuse

Delaney DiMaggio,[a] Adam T. Brockett,[b] Michael Shuster,[c] Steven Murkli,[a] Canjia Zhai,[a] David King,[a] Brona O'Dowd,[a] Ming Cheng,[a] Kimberly Brady,[a] Volker Briken,[c] Matthew R. Roesch,[b] and Lyle Isaacs*[a]

We report studies of the interaction of six acyclic CB[n]-type receptors toward a panel of drugs of abuse by a combination of isothermal titration calorimetry and ^{1}H NMR spectroscopy. Anthracene walled acyclic CB[n] host (**M3**) displays highest binding affinity toward methamphetamine ($K_d = 15$ nM) and fentanyl ($K_d = 4$ nM). Host **M3** is well tolerated by Hep G2 and HEK 293 cells up to 100 μM according to MTS metabolic and adenylate kinase release assays. An *in vivo* maximum tolerated dose study with Swiss Webster mice showed no adverse effects at the highest dose studied (44.7 mg kg^{-1}). Host **M3** is not mutagenic based on the Ames fluctuation test and does not inhibit the hERG ion channel. *In vivo* efficacy studies showed that pretreatment of mice with **M3** significantly reduces the hyperlocomotion after treatment with methamphetamine, but **M3** does not function similarly when administered 30 seconds after methamphetamine.

Introduction

Prescription and illicit drugs were implicated in 70,630 drug overdose deaths in the United States in 2019.[1] The drug abuse epidemic has been declared a national emergency by the federal government.[2] The economic costs attributed to drug abuse exceeded $271 billion in 2011 when considering health-care costs and decreased work productivity.[3] In particular, death due to overdose with opioids (e.g. fentanyl and synthetic analogues) and non-opioids (e.g. methamphetamine and cocaine) have rapidly increased in recent years which highlights the pressing need to develop new and improved therapeutics to counteract the full range of opioids and non-opioids.[4] Currently, overdose with opioids can be treated with Naloxone which exerts a pharmacodynamic effect by binding to the opioid receptor.[5] Unfortunately, Naloxone is less effective at treating patients poisoned by high potency opioids like carfentanil and is ineffective at treating overdose with non-opioids (e.g. methamphetamine, PCP, cocaine, ketamine).[6] Accordingly, researchers have been exploring different strategies to counteract the effects of drugs of abuse. One approach is the pharmacokinetic strategy which relies on a reduction of the concentration of unmodified drug in circulation.[5] For example, the catalytic transformation of cocaine into ecgonine methyl ester by human butyrylcholine esterase has been explored as a treatment for intoxication with cocaine.[7] An alternative pharmacokinetic strategy is based on antibody therapeutics which bind tightly to a specified drug (e.g. cocaine, methamphetamine, fentanyl, carfentanil)[8] in the bloodstream and thereby prevent their passage across the blood brain barrier. As part of an ongoing line of inquiry, we are exploring whether high affinity supramolecular hosts (Figure 1) are capable of *in vitro* and *in vivo* sequestration[9] of drugs of

[a] *D. DiMaggio, Dr. S. Murkli, Dr. C. Zhai, D. King, B. O'Dowd, Dr. M. Cheng, Dr. K. Brady, Prof. Dr. L. Isaacs*
Department of Chemistry and Biochemistry,
University of Maryland
College Park, MD 20742 (USA)
E-mail: LIsaacs@umd.edu
[b] *Dr. A. T. Brockett, Prof. Dr. M. R. Roesch*
Department of Psychology and Program in Neuroscience and Cognitive Science (NACS),
University of Maryland
College Park, MD 20742 (USA)
[c] *M. Shuster, Prof. Dr. V. Briken*
Department of Cell Biology and Molecular Genetics,
University of Maryland
College Park, MD 20742 (USA)

Supporting information for this article is available on the WWW under https://doi.org/10.1002/cmdc.202200046

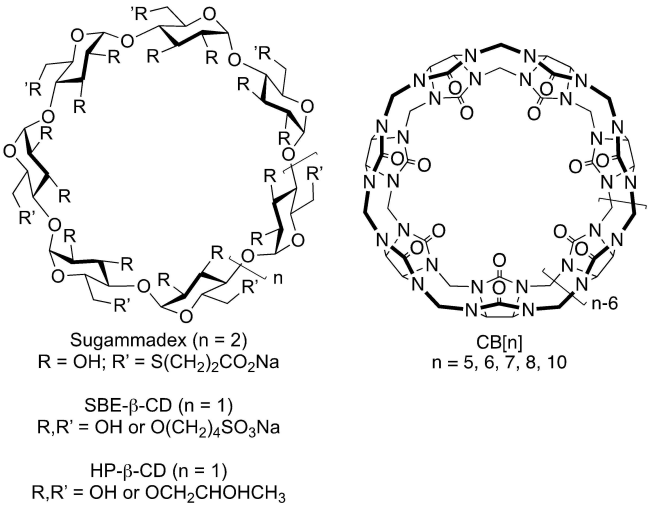

Figure 1. Structures of Sugammadex, SBE-β-CD, HP-β-CD and CB[n].

abuse, especially methamphetamine, as their host·drug complexes to combat death due to drug overdose.[10]

Over the past 50 years, supramolecular chemists have gained a deep understanding of non-covalent interactions and the principles for macrocyclic host design, and increasingly seek to create host·guest complexes that are tailored to specific chemical and biological applications.[11] Macrocyclic host systems are most popular because they typically display good levels of preorganization which results in high binding affinity and selectivity.[11a] Crown ethers, cyclodextrins, cavitands, calixarenes, cucurbiturils, cyclophanes, and most recently pillararenes constitute the most widely studied macrocyclic hosts.[11a,12] The chemical, physical, optical, and even biological properties of host·guest complexes can be very different than those of the uncomplexed guest which enables a range of applications including molecular machines,[11d,13] chiral stationary phases,[14] sensing ensembles,[15] supramolecular catalysts,[16] and household deodorizing products.[17] For macrocycles that are water soluble, biocompatible, and display good binding affinity, *in vitro* and *in vivo* applications can be envisioned. For example, the Smith group encapsulates fluorophores within tetralactam macrocycles for *in vivo* imaging applications.[18] The Liu group showed that administration of sulfonated calixarene could be used to ameliorate the toxicity of methyl viologen in mice.[19] Of highest societal impact are the cyclodextrin derivatives HP-β-CD, SBE-β-CD, and Sugammadex (Figure 1) which are used in household deodorizing products, to formulate insoluble drugs for parenteral administration, and as a post-operative reversal agent for the lingering effects of rocuronium and vecuronium.[17a,20]

We, and others, have been interested in macrocyclic CB[n] (n = 5, 6, 7, 8, 10; Figure 1)[12g,21] which display remarkably high binding affinity toward hydrophobic (di)cations in water (K_a up to 10^{17} M^{-1} in special cases) driven by a combination of ion-dipole interactions and the hydrophobic effect.[22] CB[7] has been most studied because of its decent water solubility (> 5 mM), high biocompatibility, and its ability to host a range of chemically and biologically interesting guests.[23] For example, the Wang group administered CB[7] to mice to counteract the toxicity of paraquat, to reverse general anesthesia in Zebrafish, and to decrease blood coagulation induced by hexadimethrine in mice.[24] Additionally, our group synthesized water soluble Me_4CB[8] and demonstrated that it could be used to sequester PCP *in vivo* (mice) and modulate their locomotor activity.[10c]

In recent years, we and others, have been investigating acyclic CB[n]-type receptors (e.g. **M1** and **M2**, Figure 2) which feature a central glycoluril oligomer, two aromatic sidewalls, and four $(CH_2)_3SO_3Na$ solubilizing groups.[9b,25] Acyclic CB[n] display high water solubility, excellent biocompatibility, and can be functionalized to tailor the binding affinity toward guests including insoluble drugs, neuromuscular blockers, anesthetics, and drugs of abuse (**1**–**13**, Figure 3).[10a,26] Previously, we have shown that **M1** and **M2** function as *in vivo* sequestration agents for methamphetamine and fentanyl.[10a,b] Researchers have also investigated the binding of amphetamines to HP-β-CD (meth, $K_a = 190$ M^{-1}), sulfonated calix[4]arene (meth, $K_a = 3.8\times10^4$ M^{-1}), phosphonate cavitands (MDMA, $K_a = 1.15\times10^5$ M^{-1} in CD_3OD), and CB[7] (meth, $K_a = 1.2\times10^8$ M^{-1}; 8.1×10^5 M^{-1}).[9c,10a,27] In recent papers, we showed that sulfate solubilized acyclic CB[n] (e.g. **M0**; deletion of the $(CH_2)_3$ linking groups) bring the negative charge closer to the ureidyl C=O portals and thereby give somewhat higher binding affinity toward hydrophobic (di)cations.[28] An *In vivo* efficacy study showed that the hyperlocomotion of animals that had received methamphetamine could be controlled by administration of **M0** 5 minutes later.[10d] In a separate direction, we have determined the influence of the aromatic wall of acyclic CB[n] (e.g. **Me_4M1**, **Z1**, **L1**, **M3**) on the binding affinity and found that π-extension (e.g. **M1** to **M2** to **M3**) generally enhances K_a albeit with decreased inherent solubility and increased self-association.[29] In this paper, we measure the binding affinity of six acyclic CB[n]-type receptors (**M1**, **M2**, **M3**, **Me_4M1**, **Z1**, and **L1**, Figure 2) toward a panel of drugs of abuse (**1**–**13**, Figure 3) by a single analytical method

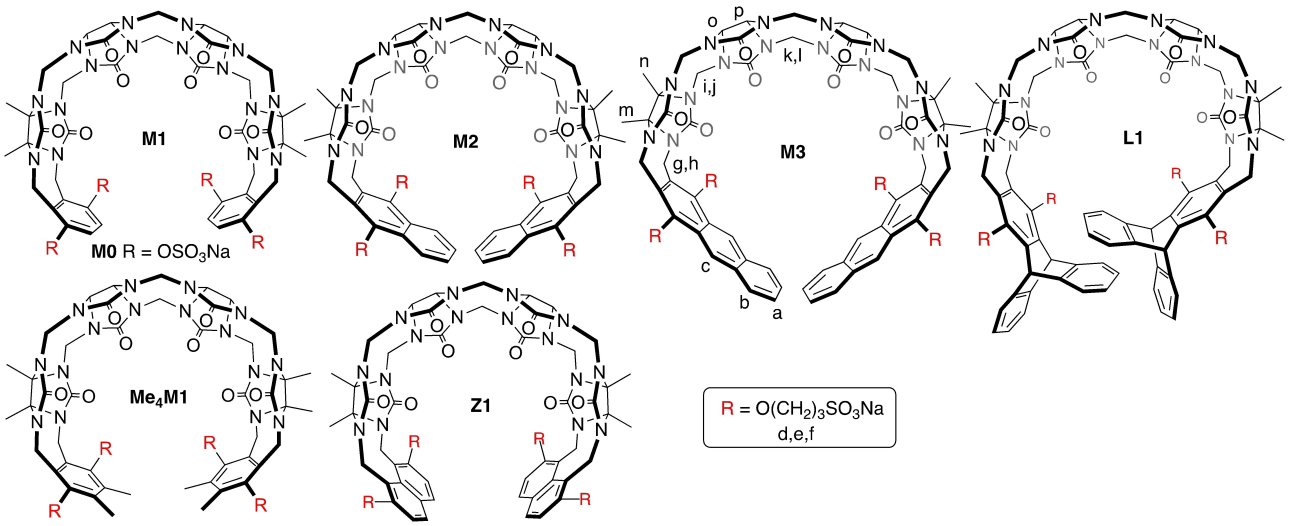

Figure 2. Structures of acyclic CB[n]-type receptors used in this study.

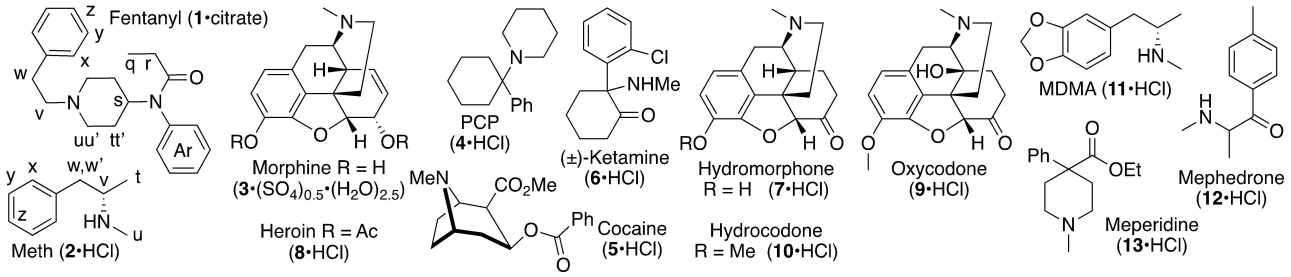

Figure 3. Structures of the drugs used in this study.

(isothermal titration calorimetry, ITC) followed by a variety of *in vitro* and *in vivo* toxicity and efficacy studies for **M3**.

Results and Discussion

This results and discussion section is organized as follows. First, we determine the binding constants of the six acyclic CB[n]-type hosts toward the drugs of abuse panel (**1**–**13**) by isothermal titration calorimetry, glean information regarding the geometry of selected host·drug complexes by ^{1}H NMR spectroscopy, and discuss trends in the structure-binding affinity dataset. Subsequently, we examine the biocompatibility of **M3** in a series of *in vitro* (cell viability, cell death, hERG ion channel inhibition, AMES fluctuation test) and *in vivo* (maximum tolerated dose) assays. Finally, we perform an *in vivo* efficacy study of the ability of **M3** to modulate the locomotor activity of mice treated with methamphetamine.

Qualitative ^{1}H NMR study of M3·drug complexes

The ^{1}H NMR spectrum recorded for **M3** (0.4 mM) in D_2O at room temperature (Figure 4d) displays highly broadened resonances. These resonances sharpen dramatically when the spectrum is recorded at 348 K or when DMSO-d_6 is used as the solvent which reflects extensive hydrophobically driven self-association of **M3**.[29] Under these conditions the spectrum shows three resonances for the substituted anthracene walls of **M3** in accord with time averaged C_{2v}-symmetry on the chemical shift timescale. Figure 4c shows the ^{1}H NMR spectrum recorded for methamphetamine whereas Figure 4b and 4a show the spectra at 1:1 and 1:2 **M3**:methamphetamine molar ratios. The resonances of the aromatic ring of methamphetamine (H_x, H_y, H_z) undergo significant upfield shifts (from ≈7.4 ppm to ≈5.8 ppm) upon formation of the **M3**·methamphetamine complex (Figure 4b) which indicates that the aromatic ring is bound within the cavity of **M3** with its magnetically shielding anthracene walls. Smaller upfield shifts are noted for methyl groups H_t and H_u which indicate that these groups reside closer to the ureidyl carbonyl portals to enable ion-dipole interactions of the ammonium ion. A similar geometry was previously noted for the **M1**·methamphetamine and CB[7]·methamphetamine complexes by x-ray crystallography.[10a] At a 1:2 **M3**·methamphetamine ratio, the resonances for H_x, H_y, H_z, H_t, and H_u (Figure 4a) shift back toward the chemical shifts observed for uncomplexed methamphetamine which indicates that the dynamics of guest exchange are fast on the ^{1}H NMR chemical shift timescale. Interestingly, the resonances for H_a, H_b, and H_c for **M3** undergo slight downfield shifts and split into pairs of resonances upon formation of the **M3**·methamphetamine complex. The changes

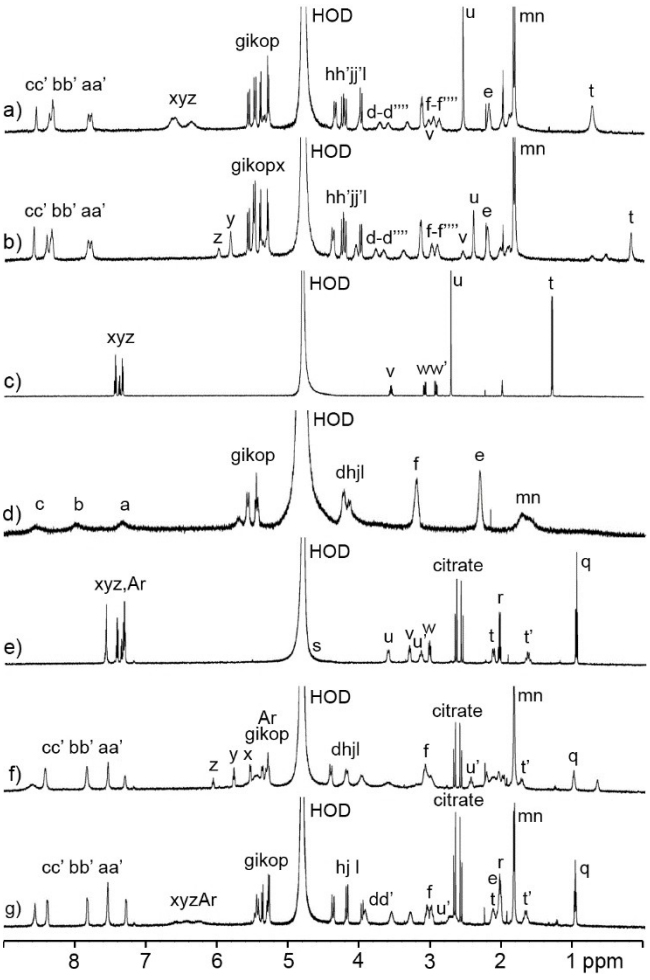

Figure 4. ^{1}H NMR spectra recorded (600 MHz, RT, D_2O) for: a) a mixture of **M3** (0.2 mM) and methamphetamine (0.4 mM), b) an equimolar mixture of **M3** and methamphetamine (0.2 mM), c) methamphetamine (0.4 mM), d) **M3** (0.4 mM), e) fentanyl citrate (0.4 mM), f) an equimolar mixture of **M3** and fentanyl (0.2 mM), and g) a mixture of **M3** (0.2 mM) and fentanyl (0.4 mM).

in chemical shift likely reflect differences in the relative orientation of the magnetically shielding anthracene walls in **M3** versus **M3**·methamphetamine; similar changes have been observed previously for **M2**·guest complexes.[26a] The presence of pairs of resonances for H_a–H_c (e.g. a, a′, b, b′, c, c′) arise because the use of chiral and enantiomerically pure methamphetamine results in a C_1-symmetric **M3**·methamphetamine complex. When guest exchange is fast on the chemical shift timescale and the ammonium ion can reside at either C=O portal the time averaged symmetry of the host is C_2-symmetric which explains the observed pairs of resonances. Similar complexation induced splitting of resonances and changes in chemical shift were observed for the **M3**·fentanyl complex as shown in Figure 4e–4 g which is not surprising given that methamphetamine and fentanyl share a common phenethyl ammonium ion binding epitope. ^{1}H NMR stack plots for other **M3**·drug complexes are given in the Supporting Information.

Measurement of the thermodynamic parameters of complex formation by ITC

After confirming that the geometry and dynamic properties of **M3**·drug complexes were in line with expectations based on drug structure and previous studies,[10a,d,28–29] we proceeded to measure the complexation thermodynamics. Given the tight binding previously observed for **M3**,[29] the limited dynamic range of ^{1}H NMR titrations ($K_a \leq 10^4$ M^{-1}),[30] and our desire to use a common analytical method for all binding constant measurements suggested the use of ITC.[31] Previously we have measured the K_a values of **M1** and **M2** toward fentanyl and hydromorphone by ITC but not for the other drugs in the panel (Figure 3).[10a] Accordingly, we measured the binding thermodynamics for all six acyclic CB[n] hosts (**M1**, **M2**, **M3**, **Me$_4$M1**, **Z1**, **L1**) by ITC in 20 mM NaH_2PO_4 buffered H_2O (pH 7.4) at 298 K. Direct ITC titrations measure the heat evolved when a solution of host in the cell is titrated with a solution of guest from the ITC syringe which can be fitted to a 1:1 binding model by the PEAQ ITC data analysis software to extract K_a, ΔH and host·guest stoichiometry. Direct ITC are appropriate and accurate when the c-value ($c = K_a \times [host]$) is less than 500 which corresponds to $K_a \leq 5 \times 10^6$ M^{-1} when the fixed concentration of host is 100 μM.[31–32] Accordingly, we measured the host·drug complexes **M1**, **M2**, **Me$_4$M1**, **Z1**, and **L1** by direct ITC titrations (Supporting Information); the K_a and ΔH values are reported in Table 1. For host **M3** which is self-associated in water at the 100 μM concentrations used for ITC, it was necessary to perform competitive ITC titrations to eliminate the effects of self-association.[33] As described previously,[29] we first measured the K_a and ΔH values for a weak binding competitor at elevated temperatures where self-association is minimized and extrapolated the values back to 298 K which are then used as inputs for the competitive binding experiment. Previously, we found that butanediammonium dichloride is an appropriate competitor

Table 1. Binding constants (K_a, M^{-1}) and enthalpies (ΔH, kcal mol^{-1}) of complexation determined for hosts (**M1**, **M2**, **M3**, **Me$_4$M1**, **Z1**, **L1**) with the panel of drugs of abuse (**1**–**13**) by direct and competition ITC titrations. Conditions: 20 mM NaH_2PO_4 buffered water (pH = 7.4), 298 K.

G	M1 K_a [M^{-1}] $\Delta H°$ [kcal/mol]	Me$_4$M1 K_a [M^{-1}] $\Delta H°$ [kcal/mol]	M2 K_a [M^{-1}] $\Delta H°$ [kcal/mol]	M3 K_a [M^{-1}] $\Delta H°$ [kcal/mol]	Z1 K_a [M^{-1}] $\Delta H°$ [kcal/mol]	L1 K_a [M^{-1}] $\Delta H°$ [kcal/mol]
1 (fentanyl)	$(1.10 \pm 0.40) \times 10^{7}$[a] -20.9 ± 0.06	$(1.15 \pm 0.05) \times 10^{6}$ -10.8 ± 0.05	$(7.60 \pm 0.50) \times 10^{6}$[a] -20.2 ± 0.07	$(2.54 \pm 0.29) \times 10^{8}$[c] -19.1 ± 0.25	$(3.94 \pm 0.10) \times 10^{5}$ -9.58 ± 0.04	$(1.11 \pm 0.05) \times 10^{6}$ -11.3 ± 0.07
2 (Meth)	$(1.47 \pm 0.06) \times 10^{6}$[b] -11.2 ± 0.02	$(6.94 \pm 0.45) \times 10^{5}$ -8.99 ± 0.08	$(2.00 \pm 0.10) \times 10^{6}$[b] -10.0 ± 0.04	$(6.66 \pm 0.65) \times 10^{7}$[c] -14.8 ± 0.21	$(8.40 \pm 0.61) \times 10^{4}$ -9.73 ± 0.22	$(1.02 \pm 0.09) \times 10^{6}$ -12.6 ± 0.17
3 (morphine)	$(6.29 \pm 0.05) \times 10^{5}$[b] -13.0 ± 0.18	$(1.74 \pm 0.09) \times 10^{5}$ -11.5 ± 0.14	$(2.15 \pm 0.81) \times 10^{6}$[b] -12.8 ± 0.73	$(6.02 \pm 0.01) \times 10^{6}$[d] -12.9 ± 0.13	$(2.29 \pm 0.22) \times 10^{4}$ -8.88 ± 0.24	$(2.03 \pm 0.04) \times 10^{4}$ -15.0
4 (PCP)	$(6.25 \pm 0.36) \times 10^{4}$[b] -6.08 ± 0.13	$(3.46 \pm 0.61) \times 10^{4}$ -2.24 ± 0.20	$(3.48 \pm 0.20) \times 10^{5}$[b] -6.08 ± 0.07	$(1.22 \pm 0.01) \times 10^{6}$[d] -7.41 ± 0.15	$(4.26 \pm 0.58) \times 10^{4}$ -4.28 ± 0.19	$(1.00 \pm 0.03) \times 10^{6}$ -9.14 ± 0.03
5 (cocaine)	$(4.04 \pm 0.39) \times 10^{5}$[b] -11.0 ± 0.07	n.b.	$(5.21 \pm 0.77) \times 10^{5}$[b] -17.4 ± 0.46	$(2.50 \pm 0.1) \times 10^{6}$[e] -15.8 ± 0.02	$(1.49 \pm 0.27) \times 10^{4}$ -11.2 ± 0.9	$(1.14 \pm 0.39) \times 10^{5}$ -10.9 ± 0.10
6 (ketamine)	$(1.19 \pm 0.21) \times 10^{4}$[b] $-6.95 \pm .99$	$(6.99 \pm 0.80) \times 10^{4}$ $-2.03 \pm .09$	$(3.70 \pm 0.47) \times 10^{5}$[b] $-13.6 \pm .03$	$(1.00 \pm 0.02) \times 10^{6}$[e] -12.1 ± 0.02	n.b.	$(7.09 \pm 0.22) \times 10^{4}$ -12.7 ± 0.13
7 (hydromorph)	$(1.80 \pm 0.03) \times 10^{5}$[a] -11.20 ± 0.04	n.d.	$(6.80 \pm 0.10) \times 10^{5}$[a] -12.1 ± 0.03	$(1.05 \pm 0.01) \times 10^{6}$[d] -13.6 ± 0.08	n.d.	n.d.
8 (heroin)	$(3.82 \pm 0.65) \times 10^{5}$ -14.0 ± 0.04	$(1.62 \pm 0.03) \times 10^{5}$ -27.6 ± 0.11	$(5.29 \pm 0.89) \times 10^{5}$ -17.7 ± 0.04	n.d.	$(6.62 \pm 1.21) \times 10^{3}$ -7.49 ± 0.73	$(2.31 \pm 0.21) \times 10^{4}$ -12.8 ± 0.68
9 (oxycodone)	$(1.76 \pm 0.04) \times 10^{5}$ -11.9 ± 0.07	$(3.27 \pm 0.22) \times 10^{5}$ -8.48 ± 0.10	$(1.16 \pm 0.03) \times 10^{6}$ -14.8 ± 0.04	n.d.	$(6.25 \pm 0.55) \times 10^{3}$ -5.77 ± 0.21	$(5.85 \pm 0.35) \times 10^{4}$ -11.6 ± 0.26
10 (hydrocodone)	$(1.67 \pm 0.53) \times 10^{5}$ -10.5 ± 0.08	$(2.54 \pm 0.24) \times 10^{5}$ -11.8 ± 0.24	$(1.82 \pm 0.16) \times 10^{6}$ -15.5 ± 0.17	n.d.	$(1.16 \pm 0.03) \times 10^{4}$ -6.40 ± 0.09	$(4.20 \pm 0.28) \times 10^{4}$ -12.4 ± 0.34
11 (MDMA)	$(1.13 \pm 0.36) \times 10^{6}$ -15.0 ± 0.06	$(4.52 \pm 0.02) \times 10^{6}$ -8.84 ± 0.07	$(1.00 \pm 0.07) \times 10^{7}$ -17.7 ± 0.12	n.d.	$(1.28 \pm 0.07) \times 10^{5}$ -10.4 ± 0.2	$(8.00 \pm 0.02) \times 10^{5}$ -15.1 ± 0.09
12 (mephedrone)	$(5.15 \pm 0.42) \times 10^{5}$ -11.3 ± 0.16	$(1.00 \pm 0.06) \times 10^{6}$ -11.6 ± 0.10	$(5.05 \pm 0.29) \times 10^{6}$ -13.7 ± 0.07	n.d.	$(8.26 \pm 0.53) \times 10^{4}$ -11.1 ± 0.2	$(7.87 \pm 0.23) \times 10^{5}$ -13.0 ± 0.05
13 (meperidine)	$(1.95 \pm 0.45) \times 10^{4}$ -2.51 ± 0.37	$(1.20 \pm 0.09) \times 10^{4}$ -8.92 ± 0.36	$(2.34 \pm 0.36) \times 10^{4}$ -4.10 ± 0.34	n.d.	$(1.23 \pm 0.31) \times 10^{3}$ -6.15 ± 1.39	$(1.42 \pm 0.15) \times 10^{5}$ -4.43 ± 0.13

[a] Taken from the literature.[10a] [b] Determined here by ITC but previously reported by UV/Vis titration.[10a,26c,34] [c] Determined by competition ITC using $H_2N(CH_2)_4NH_2 \cdot 2HCl$ as competitor. [d] Determined by competition ITC using hexamethyl-*p*-xylenediammonium·2I$^-$ as competitor. [e] Determined by competition ITC using $Me_3N(CH_2)_6NMe_3 \cdot 2I^-$ as competitor. n.d. = not determined. n.b. = no heat evolved.

($K_a = 6.31 \times 10^5\ M^{-1}$; $\Delta H = -6.51$ kcal mol^{-1}) to use when determining higher binding constants with **M3**.[29] In the competitive ITC titration a solution of **M3** and an excess of butanediammonium dichloride in the ITC cell, which ensures that **M3** is not aggregated, is titrated with a solution of the tighter binding guest (e.g. methamphetamine, Figure 5a) from the ITC syringe. As shown in Figure 5b, the peaks in the thermogram are integrated and plots of ΔH versus molar ratio are fitted to a competitive binding model to extract K_a and ΔH for the **M3**·methamphetamine complex ($K_a = (6.66 \pm 0.65) \times 10^7\ M^{-1}$ and $\Delta H = -14.8 \pm 0.21$ kcal mol^{-1}). The K_a values for the remaining **M3**·guest complexes were determined by competition ITC (Supporting Information) and are reported in Table 1.

The binding constants given in Table 1 span over 5 orders of magnitude from $1.23 \times 10^3\ M^{-1}$ (**Z1**·mepiridine) to $2.54 \times 10^8\ M^{-1}$ (**M3**·fentanyl). Accordingly, a discussion of the trends in the thermodynamic data is appropriate. All of the complexation events are driven by favorable enthalpic changes due to the operation of the non-classical hydrophobic effect.[35] The non-classical hydrophobic effect derives in part from the presence of intracavity waters that lack a full complement of H-bonds that are released to bulk water upon complexation. Previous workers have documented the non-classical hydrophobic effect using cyclophane and macrocyclic CB[n] hosts.[35] Hosts **M1**, **M2**, and **M3** form a homologous series that differ in the length of the aromatic walls.[29] This structural change results in larger cavity sizes for the longer walled hosts which in turn results in larger numbers of intracavity waters in the uncomplexed host that can be released upon complexation. A perusal of Table 1 shows that the binding affinities toward a specific drug generally show the following trend: **M1** < **M2** < **M3**. For example, methamphetamine binds to **M1** ($1.47 \times 10^6\ M^{-1}$), **M2** ($2.00 \times 10^6\ M^{-1}$), and **M3** ($6.66 \times 10^7\ M^{-1}$) in accord with this trend as do morphine, PCP, cocaine, ketamine, and hydromorphone. The walls of **Me$_4$M1** are longer than **M1** and shorter than **M2** but also differ in that the hydrophobic sp^3-hybridized Me groups change the makeup of the surfaces contacting the guest and perhaps the nature of the interaction between the tips of the uncomplexed receptor. Nevertheless, Table 1 shows that **Me$_4$M1** always binds less tightly than **M2** to a given drug and that **M1** and **Me$_4$M1** generally bind with comparable affinities (K_a (**Me$_4$M1**·drug)/K_a (**M1**·drug) range from 0.1 to 5.9. Host **Z1** is an isomer of **M2** with deeper rather than longer walls. Table 1 establishes that **Z1** is the least potent host studied toward nearly all guests with K_a values ranging from 1230 to $4.07 \times 10^5\ M^{-1}$. In agreement with these results, we have previously observed that **Z1** is a poor solubilizing excipient for insoluble drugs which was traced to its poor binding affinities.[36] Finally, triptycene derived host **L1** is similar to **M3** in that its cavity is shaped by three 6-membered rings per wall but in a curved rather than a linear fashion. Previously, we showed that **L1** undergoes a self-folding process that reduces the overall cavity volume.[37] Accordingly, **L1** is always less potent than **M3** toward a given drug with (K_a (**M3**·drug)/K_a (**L1**·drug) ranging from 1.2 to 296. In fact, the binding abilities of **L1** are more comparable to **M1** with (K_a (**M1**·drug)/K_a (**L1**·drug) ranging from 0.06 to 31. We can also compare the affinities of each host individually toward all 13 members of the drug panel (Table 1). We find that fentanyl, methamphetamine, MDMA, and mephedrone are generally the tightest binders to a specific host. This result can be understood based on the preferred binding determinants of CB[n]-type receptors which include a purely hydrophobic residue adjacent to a cationic center.[9b,21a,22b] The phenethyl ammonium ion moieties of fentanyl, methamphetamine, MDMA, and mephedrone allow optimization of both interactions. Conversely, drugs with the morphinan ring system (e.g. **3**, **7**–**10**) generally bind more weakly – despite the phenethylammonium ion moiety due to the bulkiness of the ring system which prevents simultaneous optimization of the hydrophobic effect and ion-dipole interactions. In addition, the residual intracavity solvation of the three or four O-atoms of the morphinan ring system likely reduces binding affinity for this class of compounds. Overall, Table 1 establishes that **M3** is the most powerful host toward the drugs studied including the non-opioid methamphetamine which cannot be counteracted by the use of naloxone. Accordingly, we decided to proceed toward the use of **M3** as an *in vivo* reversal agent for methamphetamine.

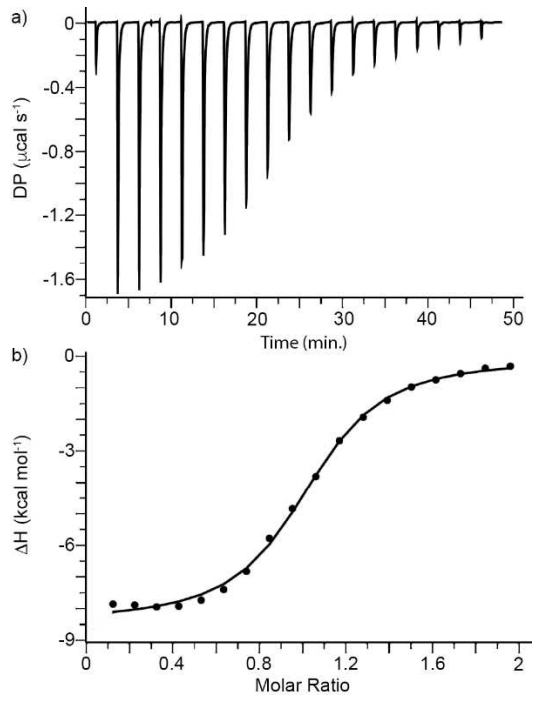

Figure 5. a) Plot of DP vs time from the titration of **M3** (100 μM) and $ClH_3N(CH_2)_4NH_3Cl$ (500 μM) in the cell with methamphetamine (1.02 mM) in the syringe in 20 mM NaH_2PO_4 buffer (pH = 7.4). b) Plot of ΔH as a function of molar ratio of **M3** to methamphetamine. The solid line represents the best non-linear fit of the data to a competitive binding model with $K_a = (6.66 \pm 0.65) \times 10^7\ M^{-1}$ and $\Delta H = (-14.8 \pm 0.21)$ kcal mol^{-1}.

Cytotoxicity and maximum tolerated dose studies conducted for M3

The high affinity of **M3** toward methamphetamine ($K_d = 15$ nM) and fentanyl ($K_d = 4$ nM) encouraged us to verify the *in vitro* and

in vivo compatibility of **M3** as a prelude to *in vivo* efficacy studies. Figure 6 shows the results of cell viability (MTS) and cell death (adenylate kinase (AK) release) assays performed for **M3**. Human embryonic kidney and human liver cells (HEK 293, CRL-1573; Hep G2, HB-8065, purchased from ATCC) were used because compounds are processed and cleared by these organs which are therefore potential sites of toxicity. In the AK release assay distilled water was used as positive control (100% release) whereas in the MTS assay untreated (UT) cells were set to 100% cell viability. Figures 6a and 6b show that treatment of HEK 293 or Hep G2 cells with **M3** at concentrations up to 100 μM for 24 hours gives cell viability levels that are not statistically significantly different than untreated control cells. However, at higher concentrations (300 μM) statistically significantly lower levels of cell viability were observed. Figures 6c and 6d establish that treatment with **M3** at the highest dose (300 μM) showed very low levels of cell death relative to distilled water treatment. These results establish the acceptable cytotoxicity profile of **M3**.

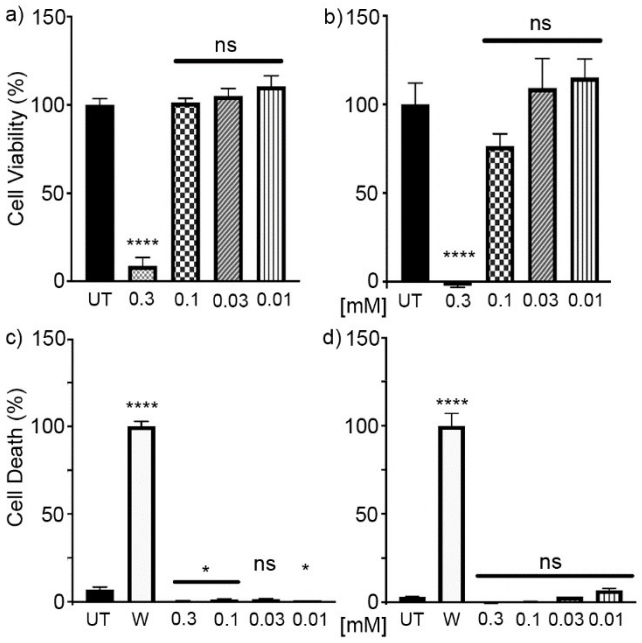

Figure 6. *In vitro* cytotoxicity experiments performed for **M3**. a) Hep G2 cell viability assay after incubating the cells with **M3** for 24 h. b) HEK 293 cell viability assay performed after incubation with **M3** for 24 h. c) Hep G2 cell death after incubation with **M3**. d) HEK 293 cell death after incubation with **M3**. The AK assays in panels c and d were performed using the supernatant from cells seeded for MTS assay. All panels of the figure show the average and SEM values from two replicate experiments. Statistical analysis is one-way ANOVA with Dunnett's multiple comparisons test. UT = untreated; *P = 0.01–0.05; **P = 0.001–0.01; ***P = 0.001 −0.0001; ****P < 0.0001.

After establishing the good cytocompatibility of **M3** at concentrations up to 100 μM, we moved on to *in vivo* maximum tolerated dose studies (Figure 7). All animal experiments were approved by the Animal Care and Use Committee at the University of Maryland (R-JAN-17-25 and R-AUG-18-42) and followed the guidelines of the National Research Council committee for the Update of the Guide for the Care and Use of Laboratory Animals. For the *in vivo* MTD study, **M3** was formulated in normal phosphate buffered saline (PBS). A total of 20 female Swiss Webster mice were used and divided into four groups (PBS only (n = 5), 12.3, 23.9, and 44.7 mg/kg **M3** (each n = 5)). The animals were dosed on days 0 and 2 (denoted with *) via tail vein injection (0.150 mL) and their weight and health status were recorded every other day until day 16. Figure 7 shows that the weights of the mice receiving the highest dose (44.7 mg/kg) are very similar to those receiving PBS as control. Furthermore, the mice did not show any signs of adverse behaviors (e.g. labored breathing, reduced locomotion) after dosing. Accordingly, we continued in our workflow toward the evaluation of the *in vivo* efficacy of **M3** to sequester methamphetamine.

M3 Does Not Inhibit the hERG Ion Channel. The hERG ion channel which plays an important role in cardiac repolarization is a voltage-gated potassium ion channel. Inhibition of the hERG ion channel results in extension of the electrical depolarization and repolarization of the heart ventricles which can lead to fatal cardiac events. For this reason, the hERG ion channel inhibition assay is a key component of early drug development efforts.[38] Figure 8 shows the results of the hERG ion channel inhibition assay performed using the patch-clamp technique (QPatch HTX) at six concentrations of **M3** ranging

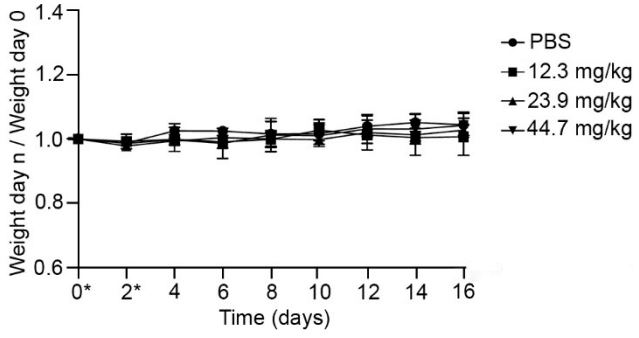

Figure 7. MTD study performed for **M3**. Female Swiss Webster mice ($n = 5$ per group) were dosed via tail vein injection (0.150 mL) on days 0 and 2 (denoted by *) with **M3** or PBS control. The normalized average weight change per study group is indicated. Error bars represent SEM.

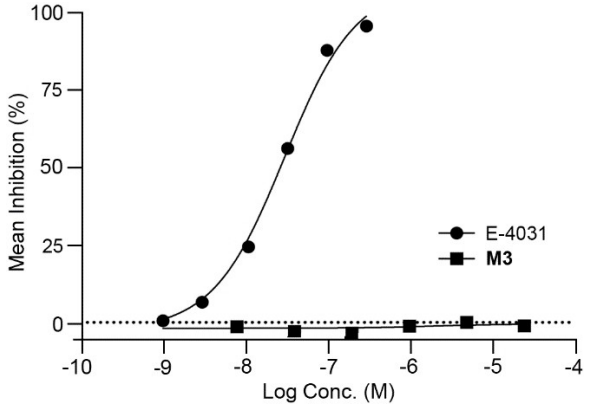

Figure 8. M3 does not inhibit the hERG ion channel. The hERG assay was conducted using HEK 293 cells stably transfected with hERG cDNA in an automated QPatch HTX patch clamp study. Plot of mean hERG ion channel inhibition (%, n = 3–4) versus log concentration for E-4031 (·) and **M3** (■).

from 0.008 μM to 25 μM along with the known hERG ion channel inhibitor E-4031. The assay was performed using mammalian cells (HEK 293) expressing the hERG ion channel. As expected, the hERG ion channel is inhibited by E-4031 at nanomolar concentrations whereas no concentration dependent inhibition is observed for **M3** at concentrations up to 25 μM. The calculated IC50 value for E-4031 is 267 nM whereas for **M3** the IC50 is higher than 25 μM. Compounds with hERG ion channel inhibition IC50 values below 100 nM are classified as highly potent whereas those with IC50 values above 10 μM are categorized as having little to no inhibitory activity.[39] Given the lack of hERG ion channel inhibition activity of **M3** we proceeded to test the mutagenicity of **M3**.

M3 is not mutagenic according to the Ames fluctuation test

The Ames fluctuation test and auxiliary bacterial cytotoxicity assays were performed to determine whether **M3** is mutagenic. The Ames fluctuation test is a reverse mutation assay that uses four S. typhimurium strains (TA98, TA100, TA1535, TA1537) which display unique mutations in the histidine operon.[40] If a compound induces a reverse mutation then the S. typhimurium strain will grow and can be quantified spectroscopically. Strain TA1535 contains a T to C missense mutation in the hisG gene (his G46) leading to a leucine to proline amino acid substitution. With the reversal of this mutation, TA1535 can detect compounds that cause base pair mutations. Strain TA1537 detects compounds that induce a +1 frameshift mutation on the his C gene (his C3076). This allows frameshift mutagens to be detected. The TA98 strain detects +1 frameshift mutation on the his D gene (his D3052) and also contains the pkM101 plasmid, which increases the sensitivity of the strain to mutagenic compounds. Finally, TA100 contains the same mutation as TA1535 plus the pkM101 plasmid. Rat liver enzyme fractions (S9) are also included in the assay to assess the potential mutagenicity of metabolites produced from the test compound.

First, to eliminate the possibility of false negatives in the Ames fluctuation test, bacterial cytotoxicity assays (Supporting Information) were performed to establish that **M3** was not cytotoxic toward the histidine revertant tester strains (TA98R, TA100R, TA1535R, TA1537R). The four tester strains were cultured overnight at 37 °C in media containing Davis Mingoli salts, D-glucose, D-biotin, and low level histidine at pH 7.0 yielding OD_{650} from 0.60 to 1.10. The cultures were then incubated with **M3** (0.6, 1.2, 2.5, 5, 10, 25, 50, 100 μM; $n=3$) for 96 hours and then OD_{650} was measured. Compounds with OD_{650} values $\leq 60\%$ of control (not treated with **M3**) are deemed cytotoxic and do not proceed to the Ames fluctuation test. The known cytotoxic compound mitomycin C ($IC_{50} \leq 100$ nM toward the tester strains) is used as a positive control. **M3** did not exhibit bacterial cytotoxicity at concentrations up to 100 μM (Supporting Information) in any of the four strains. Next, the Ames fluctuation test was performed for **M3** by incubating the culture described above in the absence and the presence of **M3** (5, 10, 50, 100 μM; $n=48$) for 96 hours with and without Arochlor-induced rat liver S9 fraction (0.2 mg mL^{-1}). Bromocresol purple is included as a colorimetric pH indicator that responds to the pH drop resulting from bacterial growth upon reverse mutation. After 96 hours, OD_{430} and OD_{570} are measured and the number of positive wells with $OD_{430}/OD_{570} \geq 1$ is determined as surrogate for reverse mutation. The statistical significance of the number of positive wells when **M3** present versus the control group (**M3** absent) is calculated using the one-tailed Fisher's exact test and classified as follows: $p < 0.001$ (very strong positive, +++); $0.001 < p < 0.01$ (strong positive, ++); $0.01 < p < 0.05$ (weak positive, +); $p > 0.05$ (negative, −). Positive control compounds that induce reverse mutation [2-aminoanthracene (2-AA), 9-aminoacridine (9-AA), Quercetin (Quer.), Streptozotocin (Strept.)] were also tested and their expected mutagenicity was confirmed (Table 2). Table 2 presents the results of the Ames fluctuation test. Compared to background, treatment with **M3** up to 100 μM does not result in a statistically significant increase in the number of positive

Table 2. Results from the Ames fluctuation test conducted for **M3**.

	TA98		TA100		TA1535		TA1537	
M3 (μM)	−S9	+S9	−S9	+S9	−S9	+S9	−S9	+S9
0	0/48	1/48	0/48	4/48	0/48	0/48	1/48	0/48
5	0/48	0/48	1/48	0/48	0/48	1/48	1/48	0/48
	–	–	–	–	–	–	–	–
10	0/48	0/48	0/48	0/48	0/48	2/48	0/48	1/48
	–	–	–	–	–	–	–	–
50	0/48	0/48	0/48	3/48	0/48	0/48	0/48	1/48
	–	–	–	–	–	–	–	–
100	0/48	1/48	0/48	0/48	0/48	0/48	0/48	0/48
	–	–	–	–	–	–	–	–
Strept.	0/48	0/48	5/48	7/48	16/48	24/48	1/48	1/48
	–	–	+	–	+++	+++	–	–
2-AA	0/48	13/48	0/48	11/48	0/48	9/48	0/48	6/48
	–	+++	–	+	–	++	–	+
Quer.	5/48	10/48	0/48	5/48	1/48	0/48	1/48	5/48
	+	+++	–	–	–	–	–	+
9-AA	0/48	0/48	0/48	2/48	0/48	0/48	24/48	24/48
	–	–	–	–	–	–	+++	+++

wells. We conclude that **M3** does not significantly increase the rate of reverse mutation and is not genotoxic.

Use of M3 to control the locomotion of mice

The high affinity of the **M3**·methamphetamine complex (K_d = 15 nM) and the good biocompatibility results for **M3** lead us to investigate whether **M3** could be used to control the biological effects of methamphetamine in mice. We capitalized on the well-known hyperlocomotive effects observed for mice treated with methamphetamine (0.5 mg/kg)[41] which can be monitored by open-field tests.[42] For these experiments, Swiss Webster mice were surgically implanted with jugular catheters featuring head mounted ports as described previously (Supporting Information).[10c] Following surgery, the animals were given 7 days to recover followed by the testing schedule given in Figure 9a. On day 1, animals were placed in the behavioral box without treatment to establish baseline locomotion levels. In each 50 minute session, the locomotion of the mouse was monitored by video and quantified by the total number of beam breaks across each session. Sessions were conducted on days 2–7 where each mouse received one of six experimental conditions (Vehicle (5% aq. Dextrose, D5 W), only methamphetamine (0.5 mg/kg), only **M3** (43.3 mg/kg), a premixed solution of methamphetamine (0.5 mg/kg) and **M3** (43.3 mg/kg) (called premix group), **M3** (43.3 mg/kg) followed 30 seconds later by methamphetamine (0.5 mg/kg) (called 30s prevent group), and methamphetamine (0.5 mg/kg) followed 30 seconds later by **M3** (43.3 mg/kg) (called 30s Treat group). These sessions were conducted in a semi-counterbalanced manner where each animal received only one treatment per day. Locomotion counts were analyzed across treatments using one-way repeated measures ANOVA with Tukey-corrected pairwise post-hoc t-tests in GraphPad Prism and the results are presented in Figure 9b as a function of treatment group. Mixed effects analysis revealed a significant main effect of treatment ($F(6,78) = 23.29$, $p \leq 0.0001$) with Tukey-corrected post-hoc comparison showing a statistically significant increase in locomotion counts for treatment with methamphetamine against the baseline, D5 W, **M3**, premix, and 30 s prevent groups. Importantly, comparisons of locomotion counts between the baseline, D5 W, and **M3** groups showed no statistically significant differences (p's > 0.96) which establishes that treatment with **M3** alone does not influence locomotion. Mice treated with the premixed solution of **M3** and methamphetamine also show a statistically significant reduction in locomotion relative to methamphetamine alone ($p < 0.0001$) with locomotion counts similar to those of baseline ($p = 0.9874$). The 30s prevent group also showed statistically significant reduction in locomotion count relative to the methamphetamine group ($p < 0.0001$) which established that precirculating **M3** successfully sequesters at least at the 30 second timepoint. Unfortunately, treatment with **M3** 30 seconds after methamphetamine (30s treat) did not show a statistically significant difference in locomotion count compared to methamphetamine alone ($p = 0.9338$). Accordingly, we conclude that **M3** is incapable of sequestering and blocking the biological effects of precirculating methamphetamine. This disappointing result, especially in light of previous successful use of related and less tight binding acyclic CB[n]-type hosts in this application,[10a,d] highlights that increasing host·methamphetamine binding affinity should not be the main or sole developmental focus. In the case of **M3**, we speculate that the extensive self-association of **M3**[29] or its high affinity toward other compounds present *in vivo* diverted **M3** from its intended target. In addition, the relative kinetics of biodistribution of **M3** and methamphetamine from the bloodstream into other compartments (e.g. brain) may be responsible for the successful sequestration of methamphetamine in the 30s prevention but not the 30s treatment groups. Finally, the

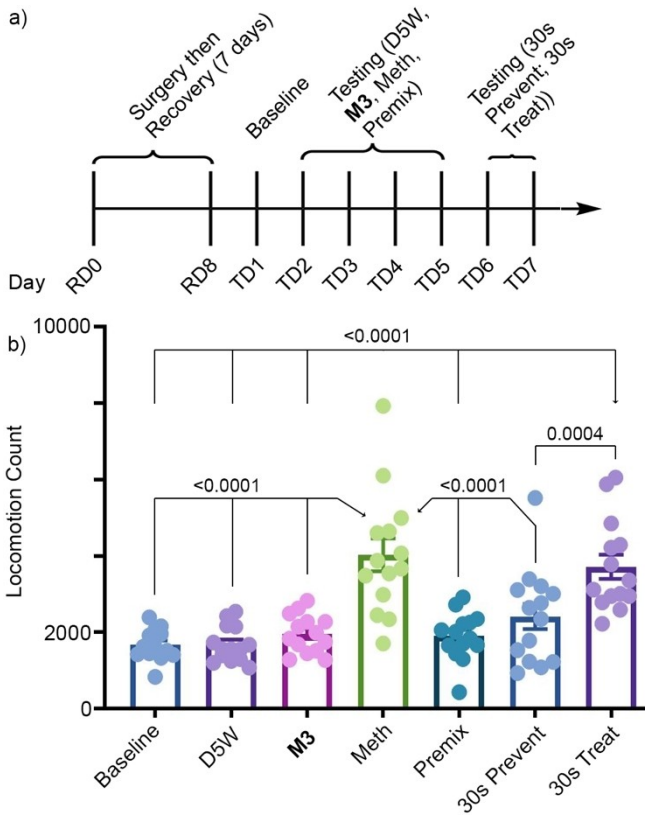

Figure 9. Efficacy study for the *in vivo* reversal of methamphetamine induced hyperlocomotion in mice. Average locomotion counts for male Swiss Webster mice (n = 14; avg weight (g) ± SD: 35.79 ± 2.12) are plotted as a function of treatment. All mice underwent an initial habituation to determine baseline locomotion levels before treatment. Following this baseline measure, treatment order was counterbalanced across days, and mice only received one treatment per day. Over six consecutive days of testing mice each received a single treatment of D5 W (0.2 mL infused), **M3** only (43.3 mg/kg; 5 mM; 0.178 mL infused), methamphetamine only (Meth; 0.5 mg/kg; 0.022 mL infused), a premixed solution of **M3** and methamphetamine (Premix; 43.3 mg/kg/0.5 mg/kg **M3**:Meth; **M3**:meth molar ratio = 9.2 : 1; 0.2 mL infused), **M3** followed by methamphetamine administered 30 s later (30s Blocking; **M3** (43.3 mg/kg, 0.178 mL infused then 0.5 mg/kg meth, 0.022 mL infused), and methamphetamine followed by **M3** administered 30 s later (30 s Reversal; meth (0.5 mg/kg), 0.022 mL infused then **M3** (43.3 mg/kg, 0.178 mL infused). Bars represent average locomotion counts. Error bars represent the standard error of the mean (SEM). Dots represent counts for each mouse (n = 14). Presented *p*-values are only for significant ($p < 0.05$) Tukey-corrected post-hoc comparisons.

relatively poor solubility of **M3** in appropriate vehicles (e.g. PBS or D5W) prevented the use of higher, potentially more efficacious, doses of **M3**.

Conclusion

In summary, we have investigated the molecular recognition properties of a panel of acyclic CB[n]-type hosts (**M1**, **Me_4M1**, **M2**, **M3**, **Z1**, **L1**) toward a panel of 13 drugs of abuse by a combination of ITC and ^{1}H NMR spectroscopy. We find that π-extension of the aromatic walls in the form of **M3** delivers highest affinity toward the drug panel with low nanomolar K_d values for **M3**·methamphetamine (K_d = 15 nM) and **M3**·fentanyl (K_d = 4 nM). Host **M3** was compatible with HEK 293 and Hep G2 cells up to 100 μM according to MTS cell viability and AK release cell death assays, did not inhibit the hERG ion channel, and was not mutagenic based on the Ames fluctuation test. *In vivo* maximum tolerated dose studies showed that **M3** is well tolerated up to 44.7 mg kg^{-1}. *In vivo* efficacy studies showed that mice treated with **M3** (43.3 mg kg^{-1}) 30 seconds before methamphetamine controlled the locomotion of the animals but treatment with **M3** 30 seconds after methamphetamine did not. In conclusion, these results highlight that the best performing *in vivo* sequestrants are not necessarily those with the highest binding affinities toward the drug targets, but rather that other properties like minimal self-association, high target selectivity, and high inherent solubility also play important roles.

Acknowledgements

We thank the US National Institutes of Health (GM132345) for financial support. The drugs used in this study were obtained from the Drug Supply Program of the National Institute on Drug Abuse. We acknowledge the NIH (T32GM080201) for a training grant fellowship to M.S. and the University of Maryland for summer research and Wylie dissertation fellowships to S.M. and Department of Education GAANN (P200A150033) fellowships to S.M. and K.B.

Conflict of Interest

L.I. is an inventor on patents held by the University of Maryland on biomedical applications of acyclic CB[n]-type receptors.

Data Availability Statement

The data that support the findings of this study are available in the supplementary material of this article.

Keywords: Cucurbituril · methamphetamine · hyperlocomotion · sequestration agent · molecular recognition

[1] https://www.drugabuse.gov/related-topics/trends-statistics#supplemental-references-for-economic-costs (accessed January 17, **2022**).
[2] a) *Facing Addition in America: The Surgeon General's Report on Alcohol, Drugs, and Health, 2016* https://www.surgeongeneral.gov/library/2016alcoholdrugshealth/index.html (accessed April 6, **2017**); b) *2019 National Drug Threat Assessment*. Drug Enforcement Administration, Drug Enforcement Administration Strategic Intelligence Section, U. S. Department of Justice, **2019**; c) *Surveillance Report of Drug-Related Risks and Outcomes, United States 2019*, Centers for Disease Control and Prevention, **2019**.
[3] a) *National Drug Threat Assessment 2011*. www.justice.gov/archive/ndic/pubs44/44849/44849p.pdf (accessed April 6, **2017**); b) H. G. Birnbaum, A. G. White, M. Schiller, T. Waldman, J. M. Cleveland, C. L. Roland, *Pain* **2011**, *12*, 657–667; c) C. S. Florence, C. Zhou, F. Luo, L. Xu, *Medical Care* **2016**, *54*, 901–906; d) *Behavioral Health Trends in the United States*. https://www.samhsa.gov/data/sites/default/files/NSDUH-FRR1-2014/NSDUH-FRR1-2014.pdf (accessed January 17, *2022*).
[4] https://www.drugabuse.gov/about-nida/legislative-activities/testimony-to-congress/2021/the-overdose-crisis-proposal-to-combat-illicit-fentanyl (accessed January 17, **2022**).
[5] D. A. Gorelick, *Future Med. Chem.* **2012**, *4*, 227–243.
[6] P. Skolnick, *Trends Pharmacol. Sci.* **2015**, *36*, 628–635.
[7] a) C.-G. Zhan, F. Zheng, D. W. Landry, *J. Am. Chem. Soc.* **2003**, *125*, 2462–2474; b) F. Zheng, W. Yang, M.-C. Ko, J. Liu, H. Cho, D. Gao, M. Tong, H.-H. Tai, J. H. Woods, C.-G. Zhan, *J. Am. Chem. Soc.* **2008**, *130*, 12148–12155; c) M. J. Shram, O. Cohen-Barak, B. Chakraborty, M. Bassan, K. A. Schoedel, H. Hallak, E. Eyal, S. Weiss, Y. Gilgun, E. M. Sellers, J. Faulknor, O. Spiegelstein, *J. Clin. Psychopharmacol.* **2015**, *35*, 396–405.
[8] a) P. T. Bremer, A. Kimishima, J. E. Schlosburg, B. Zhou, K. C. Collins, K. D. Janda, *Angew. Chem. Int. Ed.* **2016**, *55*, 3772–3775; *Angew. Chem.* **2016**, *128*, 3836–3839; b) K. C. Collins, J. E. Schlosburg, P. T. Bremer, K. D. Janda, *J. Med. Chem.* **2016**, *59*, 3878–3885; c) A. Kimishima, C. J. Wenthur, L. M. Eubanks, S. Sato, K. D. Janda, *Mol. Pharmaceutics* **2016**, *13*, 3884–3890; d) M. Gooyit, P. O. Miranda, C. J. Wenthur, A. Ducime, K. D. Janda, *ACS Chem. Neurosci.* **2017**, *8*, 468–472; e) L. M. Eubanks, S. Blake, Y. Natori, B. Ellis, P. T. Bremer, K. D. Janda, *ACS Chem. Biol.* **2021**, *16*, 277–282.
[9] a) C.-L. Deng, S. L. Murkli, L. Isaacs, *Chem. Soc. Rev.* **2020**, *49*, 7516–7532; b) S. Ganapati, L. Isaacs, *Isr. J. Chem.* **2018**, *58*, 250–263; c) H. Yin, X. Zhang, J. Wei, S. Lu, D. Bardelang, R. Wang, *Theranostics* **2021**, *11*, 1513–1526.
[10] a) S. Ganapati, S. D. Grabitz, S. Murkli, F. Scheffenbichler, M. I. Rudolph, P. Y. Zavalij, M. Eikermann, L. Isaacs, *ChemBioChem* **2017**, *18*, 1583–1588; b) T. Thevathasan, S. D. Grabitz, P. Santer, P. Rostin, O. Akeju, J. D. Boghosian, M. Gill, L. Isaacs, J. F. Cotton, M. Eikermann, *Br. J. Anaesth.* **2020**, *125*, e140–e147; c) S. Murkli, J. Klemm, A. T. Brockett, M. Shuster, V. Briken, M. R. Roesch, L. Isaacs, *Chem. Eur. J.* **2021**, *27*, 3098–3105; d) A. T. Brockett, C. Deng, M. Shuster, S. Perera, D. DiMaggio, M. Cheng, S. Murkli, V. Briken, M. R. Roesch, L. Isaacs, *Chem. Eur. J.* **2021**, *27*, 17476–17486.
[11] a) D. J. Cram, *Angew. Chem. Int. Ed. Engl.* **1988**, *27*, 1009–1020; b) J.-M. Lehn, *Angew. Chem. Int. Ed. Engl.* **1988**, *27*, 89–112; c) C. J. Pedersen, *Angew. Chem. Int. Ed. Engl.* **1988**, *27*, 1021–1027; d) J. F. Stoddart, *Angew. Chem. Int. Ed.* **2017**, *56*, 11094–11125; *Angew. Chem.* **2017**, *129*, 11244–11277.
[12] a) C. D. Gutsche, *Acc. Chem. Res.* **1983**, *16*, 161–170; b) F. Diederich, *Angew. Chem. Int. Ed. Engl.* **1988**, *27*, 362–386; c) V. Boehmer, *Angew. Chem. Int. Ed. Engl.* **1995**, *34*, 713–745; d) R. A. Rajewski, V. J. Stella, *J. Pharm. Sci.* **1996**, *85*, 1142–1169; e) M. V. Rekharsky, Y. Inoue, *Chem. Rev.* **1998**, *98*, 1875–1917; f) M. Xue, Y. Yang, X. Chi, Z. Zhang, F. Huang, *Acc. Chem. Res.* **2012**, *45*, 1294–1308; g) S. J. Barrow, S. Kasera, M. J. Rowland, J. del Barrio, O. A. Scherman, *Chem. Rev.* **2015**, *115*, 12320–12406; h) T. Ogoshi, T.-A. Yamagishi, Y. Nakamoto, *Chem. Rev.* **2016**, *116*, 7937–8002; i) J. Murray, K. Kim, T. Ogoshi, W. Yao, B. C. Gibb, *Chem. Soc. Rev.* **2017**, *46*, 2479–2496.
[13] a) Y. H. Ko, E. Kim, I. Hwang, K. Kim, *Chem. Commun.* **2007**, 1305–1315; b) S. Kassem, T. van Leeuwen, A. S. Lubbe, M. R. Wilson, B. L. Feringa, D. A. Leigh, *Chem. Soc. Rev.* **2017**, *46*, 2592–2621.
[14] R. Sardella, F. Ianni, M. Marinozzi, A. Macchiarulo, B. Natalini, *Curr. Med. Chem.* **2017**, *24*, 796–817.
[15] a) G. Ghale, W. M. Nau, *Acc. Chem. Res.* **2014**, *47*, 2150–2159; b) M. K. Meadows, E. V. Anslyn, in *Macrocyclic and Supramolecular Chemistry: How Izatt-Christensen Award Winners Shaped the Field* (Ed. R. M. Izatt), J. Wiley and Sons, Hoboken, New Jersey, **2016**, pp. 92–126; c) B. Daly, T. S. Moody, A. J. M. Huxley, C. Yao, B. Schazmann, A. Alves-Areias, J. F.

Malone, H. Q. N. Gunaratne, P. Nockemann, A. P. de Silva, *Nat. Commun.* **2019**, *10*, 49.
[16] a) C. J. Brown, F. D. Toste, R. G. Bergman, K. N. Raymond, *Chem. Rev.* **2015**, *115*, 3012–3035; b) S. H. A. M. Leenders, R. Gramage-Doria, B. de Bruin, J. N. H. Reek, *Chem. Soc. Rev.* **2015**, *44*, 433–448; c) Y. Ueda, H. Ito, D. Fujita, M. Fujita, *J. Am. Chem. Soc.* **2017**, *139*, 6090–6093.
[17] a) Febreze Home Page. https://www.febreze.com/en-us (accessed May 5, 2020); b) Aqdot Home Page. https://aqdot.com (accessed May 6, 2020).
[18] a) D.-H. Li, B. D. Smith, *Beilstein J. Org. Chem.* **2019**, *15*, 1086–1095; b) F. M. Roland, B. D. Smith, in *Supramolecular Chemistry in Water* (Ed. S. Kubik), Wiley-VCH, Weinheim, Germany, **2019**, pp. 501–524.
[19] a) K. Wang, D.-S. Guo, H.-Q. Zhang, D. Li, X.-L. Zheng, Y. Liu, *J. Med. Chem.* **2009**, *52*, 6402–6412; b) D.-S. Guo, Y. Liu, *Acc. Chem. Res.* **2014**, *47*, 1925–1934.
[20] a) V. J. Stella, R. A. Rajewski, *Pharm. Res.* **1997**, *14*, 556–567; b) J. M. Adam, D. J. Bennett, A. Bom, J. K. Clark, H. Feilden, E. J. Hutchinson, R. Palin, A. Prosser, D. C. Rees, G. M. Rosair, D. Stevenson, G. J. Tarver, M.-Q. Zhang, *J. Med. Chem.* **2002**, *45*, 1806–1816; c) A. Bom, M. Bradley, K. Cameron, J. K. Clark, J. Van Egmond, H. Feilden, E. J. MacLean, A. W. Muir, R. Palin, D. C. Rees, M.-Q. Zhang, *Angew. Chem. Int. Ed.* **2002**, *41*, 265–270; *Angew. Chem.* **2002**, *114*, 275–280.
[21] a) E. Masson, X. Ling, R. Joseph, L. Kyeremeh-Mensah, X. Lu, *RSC Adv.* **2012**, *2*, 1213–1247; b) K. I. Assaf, W. M. Nau, *Chem. Soc. Rev.* **2015**, *44*, 394–418; c) D. Shetty, J. K. Khedkar, K. M. Park, K. Kim, *Chem. Soc. Rev.* **2015**, *44*, 8747–8761.
[22] a) W. L. Mock, N.-Y. Shih, *J. Org. Chem.* **1986**, *51*, 4440–4446; b) S. Liu, C. Ruspic, P. Mukhopadhyay, S. Chakrabarti, P. Y. Zavalij, L. Isaacs, *J. Am. Chem. Soc.* **2005**, *127*, 15959–15967; c) M. V. Rekharsky, T. Mori, C. Yang, Y. H. Ko, N. Selvapalam, H. Kim, D. Sobransingh, A. E. Kaifer, S. Liu, L. Isaacs, W. Chen, S. Moghaddam, M. K. Gilson, K. Kim, Y. Inoue, *Proc. Natl. Acad. Sci. USA* **2007**, *104*, 20737–20742; d) L. Cao, M. Sekutor, P. Y. Zavalij, K. Mlinaric-Majerski, R. Glaser, L. Isaacs, *Angew. Chem. Int. Ed.* **2014**, *53*, 988–993; *Angew. Chem.* **2014**, *126*, 1006–1011.
[23] a) V. D. Uzunova, C. Cullinane, K. Brix, W. M. Nau, A. I. Day, *Org. Biomol. Chem.* **2010**, *8*, 2037–2042; b) X. Zhang, X. Xu, S. Li, L.-H. Wang, J. Zhang, R. Wang, *Sci. Rep.* **2018**, *8*, 8819; c) J. W. Lee, S. Samal, N. Selvapalam, H.-J. Kim, K. Kim, *Acc. Chem. Res.* **2003**, *36*, 621–630; d) W. M. Nau, M. Florea, K. I. Assaf, *Isr. J. Chem.* **2011**, *51*, 559–577.
[24] a) X. Zhang, X. Xu, S. Li, L. Li, J. Zhang, R. Wang, *Theranostics* **2019**, *9*, 633–645; b) H. Chen, J. Y. W. Chan, S. Li, J. J. Liu, I. W. Wyman, S. M. Y. Lee, D. H. Macartney, R. Wang, *RSC Adv.* **2015**, *5*, 63745–63752; c) Q. Huang, Q. Cheng, X. Zhang, H. Yin, L.-H. Wang, R. Wang, *ACS Appl. Bio Mater.* **2018**, *1*, 544–548.
[25] a) D. Mao, Y. Liang, Y. Liu, X. Zhou, J. Ma, B. Jiang, J. Liu, D. Ma, *Angew. Chem. Int. Ed.* **2017**, *41*, 12614–12618; b) D. Bauer, B. Andrae, P. Gass, D. Trenz, S. Becker, S. Kubik, *Org. Chem. Front.* **2019**, *6*, 1555–1560.
[26] a) D. Ma, B. Zhang, U. Hoffmann, M. G. Sundrup, M. Eikermann, L. Isaacs, *Angew. Chem. Int. Ed.* **2012**, *51*, 11358–11362; *Angew. Chem.* **2012**, *124*, 11520–11524; b) B. Zhang, P. Y. Zavalij, L. Isaacs, *Org. Biomol. Chem.* **2014**, *12*, 2413–2422; c) D. Diaz-Gil, F. Haerter, S. Falcinelli, S. Ganapati, G. K. Hettiarachchi, J. C. P. Simons, B. Zhang, S. D. Grabitz, I. M. Duarte, J. F. Cotten, K. Eikermann-Haerter, H. Deng, N. L. Chamberlin, L. Isaacs, V. Briken, M. Eikermann, *Anesthesiology* **2016**, *125*, 333–345.
[27] a) E. Biavardi, S. Federici, C. Tudisco, D. Menozzi, C. Massera, A. Sottini, G. G. Condorelli, P. Bergese, E. Dalcanale, *Angew. Chem. Int. Ed.* **2014**, *53*, 9183–9188; *Angew. Chem.* **2014**, *126*, 9337–9342; b) Y. Jang, M. Jang, H. Kim, S. J. Lee, E. Jin, J. Y. Koo, I.-C. Hwang, Y. Kim, Y. H. Ko, I. Hwang, J. H. Oh, K. Kim, *Chem* **2017**, *3*, P641-P651; c) C. P. France, G. P. Ahern, S. Averick, A. Disney, H. A. Enright, B. Esmaeli-Azad, A. Federico, L. R. Gerak, S. M. Husbands, B. Kolber, E. Y. Lau, V. Lao, D. R. Maguire, M. A. Malfatti, G. Martinez, B. P. Mayer, M. Pravetoni, N. Sahibzada, P. Skolnick, E. Y. Snyder, N. Tomycz, C. A. Valdez, J. Zapf, *Clin. Pharmacol. Ther.* **2020**, *109*, 578–590.
[28] X. Lu, S. A. Zebaze Ndendjio, P. Y. Zavalij, L. Isaacs, *Org. Lett.* **2020**, *22*, 4833–4837.
[29] S. Murkli, J. Klemm, D. King, P. Y. Zavalij, L. Isaacs, *Chem. Eur. J.* **2020**, *26*, 15249–15258.
[30] K. A. Connors, *Binding Constants*, John Wiley & Sons, New York, **1987**.
[31] T. Wiseman, S. Williston, J. F. Brandts, L.-N. Lin, *Anal. Biochem.* **1989**, *179*, 131–137.
[32] J. Broecker, C. Vargas, S. Keller, *Anal. Biochem.* **2011**, *418*, 307–309.
[33] A. Velazquez-Campoy, E. Freire, *Nat. Protoc.* **2006**, *1*, 186–191.
[34] S. Ganapati, P. Y. Zavalij, M. Eikermann, L. Isaacs, *Org. Biomol. Chem.* **2016**, *14*, 1277–1287.
[35] a) F. Biedermann, V. D. Uzunova, O. A. Scherman, W. M. Nau, A. De Simone, *J. Am. Chem. Soc.* **2012**, *134*, 15318–15323; b) E. Persch, O. Dumele, F. Diederich, *Angew. Chem. Int. Ed.* **2015**, *54*, 3290–3327; *Angew. Chem.* **2015**, *127*, 3341–3382; c) F. Biedermann, W. M. Nau, H.-J. Schneider, *Angew. Chem. Int. Ed.* **2014**, *53*, 11158–11171; *Angew. Chem.* **2014**, *126*, 11338–11352.
[36] B. Zhang, L. Isaacs, *J. Med. Chem.* **2014**, *57*, 9554–9563.
[37] X. Lu, S. K. Samanta, P. Y. Zavalij, L. Isaacs, *Angew. Chem. Int. Ed.* **2018**, *57*, 8073–8078; *Angew. Chem.* **2018**, *130*, 8205–8210.
[38] D. C. Bell, B. Fermini, *J. Pharmacol. Toxicol. Methods* **2021**, *110*, 107072.
[39] O. Roche, G. Trube, J. Zuegge, P. Pflimlin, A. Alanine, G. Schneider, *ChemBioChem* **2002**, *3*, 455–459.
[40] a) B. A. Bridges, *Arch. Toxicol.* **1980**, *46*, 41–44; b) M. Kamber, S. Fluckiger-Isler, G. Engelhardt, R. Jaeckh, E. Zeiger, *Mutagenesis* **2009**, *24*, 359–366.
[41] a) R. A. K. Singh, T. A. Kosten, B. M. Kinsey, X. Shen, A. Y. Lopez, T. R. Kosten, F. M. Orson, *Pharmacol. Biochem. Behav.* **2012**, *103*, 230–236; b) A. L. Sharp, E. Varela, L. Bettinger, M. J. Beckstead, *Int. J. Neuropsychopharmacol.* **2015**, *18*, 1–10.
[42] R. N. Walsh, R. A. Cummins, *Psychological Bulletin* **1976**, *83*, 482–504.

Manuscript received: January 24, 2022
Revised manuscript received: March 1, 2022
Accepted manuscript online: March 3, 2022
Version of record online: March 15, 2022